CONFIDENTIAL

JUN 24 1957

NACA

RESEARCH MEMORANDUM

EFFECTS OF WING INBOARD PLAN-FORM

MODIFICATIONS ON LIFT, DRAG, AND LONGITUDINAL STABILITY

AT MACH NUMBERS FROM 1.0 TO 2.3 OF A ROCKET-PROPELLED

FREE-FLIGHT MODEL WITH A 52.5° SWEPTBACK

WING OF ASPECT RATIO 3

By Allen B. Henning

Langley Aeronautical Laboratory
Langley Field, Va.

NATIONAL ADVISORY COMMITTEE
FOR AERONAUTICS
WASHINGTON
June 19, 1957

CONFIDENTIAL

DECLASSIFIED

CONFIDENTIAL

NATIONAL ADVISORY COMMITTEE FOR AERONAUTICS

RESEARCH MEMORANDUM

EFFECTS OF WING INBOARD PLAN-FORM

MODIFICATIONS ON LIFT, DRAG, AND LONGITUDINAL STABILITY

AT MACH NUMBERS FROM 1.0 TO 2.3 OF A ROCKET-PROPELLED

FREE-FLIGHT MODEL WITH A 52.5° SWEPTBACK

WING OF ASPECT RATIO 3

By Allen B. Henning

SUMMARY

An investigation was made to determine the effects of wing inboard plan-form modifications on the lift, drag, and longitudinal characteristics of a rocket-propelled free-flight model. This model had a body of fineness ratio 17.4, a modified wing with a basic plan form swept back 52.5° and an aspect ratio of 3, and inline horizontal tail surfaces which were aerodynamically pulsed continuously throughout the flight. The wing modification consisted of extending the basic wing root chord 75 percent forward and rearward and tapering this extension to zero percent of the chord at one-half the semispan. The wing thickness was increased by 10 percent at the center-line root chord. The increase of the inboard chord along with an increase of the inboard thickness increased the exposed wing volume by 70 percent over that of the basic wing. This investigation covered the Mach number range from 1.0 to 2.3. Zero-lift drag and drag due to lift were obtained during the coasting portion of the flight. Normal force, pitching moment, and longitudinal stability were measured throughout both the power-on and power-off portions of the flight.

The flight-test results which were based on the basic wing area indicate that the addition of inboard chord-extensions reduced the minimum drag and increased the lift of the configuration over that of the basic wing throughout the Mach number range. An appreciable reduction in drag due to lift was noted at Mach numbers above 1.6.

INTRODUCTION

One of the prime factors in the design of aircraft is to combine the component parts into an aerodynamically smooth configuration that produces the largest amount of lift for the least amount of drag. An example of this is shown in reference 1 where various wing-body combinations using several wing plan forms were tested to obtain their lift-drag ratios. Minor changes to the wing in a wing-body combination can produce higher lift-drag ratios. For instance, changing the leading-edge suction by changing the tip design as in reference 2 or cambering and twisting the wing as in references 3, 4, and 5 influence the lift-drag ratio. The effects of plan form, thickness ratio, thickness distribution, leading-edge radius, aspect ratio, and fuselage interference on the drag due to lift are illustrated in references 6 and 7. The influence of thickness ratio and thickened root section on the drag due to lift and maximum lift-drag ratio are demonstrated in reference 8. References 9 and 10 present the idea of inboard chord-extensions and show the effects of the extensions on the drag due to lift. The purpose of the present investigation was to determine the effect of a wing plan-form modification on drag due to lift at supersonic speeds.

For the present test, the basic swept-wing configuration of reference 11 was modified by the inboard chord extension idea. The basic model center-line root chord was extended three-fourths of the root chord forward and three-fourths rearward, tapering to zero percent extension of the local chord at one-half the semispan. Contrary to references 9 and 10 where the inboard chords were extended without increasing the wing thickness, the extended chord wing thickness of the present model was increased so that the thickness ratio was 2 percent at the wing-body juncture.

The results presented herein are part of a supersonic research program using rocket-propelled free-flight models to investigate the effect of wing configuration on lift, drag due to lift, and longitudinal stability characteristics. The model was flight tested at the Langley Pilotless Aircraft Research Station at Wallops Island, Va.

SYMBOLS

In order to have the data of the test model comparable to that of the reference models all coefficients used herein are based on the basic wing area of 4 square feet and the basic mean aerodynamic chord of 1.33 feet.

CONFIDENTIAL

a_n normal acceleration, ft/sec^2

a_l longitudinal acceleration, ft/sec^2

b wing span, ft

$\bar{c}$ wing mean aerodynamic chord of basic model, ft

C_c chord-force coefficient, $\dfrac{-a_l}{g}\dfrac{W}{qS}$

C_N normal-force coefficient, $\dfrac{a_n}{g}\dfrac{W}{qS}$

C_L lift coefficient, $C_N \cos \alpha - C_c \sin \alpha$

C_D drag coefficient, $C_c \cos \alpha + C_N \sin \alpha$

C_m pitching-moment coefficient, $\dfrac{I_Y \ddot{\theta}}{57.3 qS\bar{c}}$

g acceleration due to gravity, ft/sec^2

I_Y moment of inertia in pitch, $slug\text{-}ft^2$

M Mach number

q dynamic pressure, lb/sq ft

R Reynolds number, based on a length of 1 foot

S total wing area of basic model, sq ft

W weight of model, lb

y lateral distance from fuselage center line, ft

θ/L streamwise wing twist due to 1-pound load at 0.50 chord, deg/lb

α angle of attack, deg

β angle of sideslip, deg

$\ddot{\theta}$ angular acceleration in pitch determined from two accelerometers, $radians/sec^2$

δ   horizontal-tail deflection, deg

Subscripts:

e   elastic wing

r   rigid wing

MODEL

The wing-body-tail configuration of reference 11 was used as a basis for the present test model. The wing of the reference model or the basic wing model was modified by the addition of inboard chord-extensions. These extensions increased the center-line root chord length 75 percent forward and 75 percent rearward and tapered to zero percent extension of the local chord at the lateral wing location of one-half the semispan. The center-line wing root thickness was increased 10 percent. The increased length of the inboard chords along with the increase in thickness permitted approximately a 70-percent increase in volume in the exposed portion of the wing. The modified wing had an aspect ratio of 1.85 and was swept back 52.5° at the basic-wing quarter-chord line. The streamwise airfoil section of the inboard half of the wing varied from an NACA 65A002 at the wing-body juncture to an NACA 65A004 at one-half the semispan, whereas the outboard half of the wing had a constant airfoil section of NACA 65A004. The fuselage had a fineness ratio of 17.4. A drawing of the test model showing the location of its component parts is presented as figure 1. Photographs of the model are shown as figure 2. The ordinates of the nose section are given in table I, and the geometric and mass characteristics of the test model are presented in table II. Some characteristics of the basic wing are also included in table II.

The fuselage was of metal construction and contained a rocket motor and a telemetering system with instruments to measure the angle of attack, angle of sideslip, total pressure, and various accelerations. The aluminum-alloy wing and tail were mounted on the fuselage center line. The aerodynamically pulsed horizontal tail (ref. 12) was mass balanced and pivoted about the 55-percent point of the mean aerodynamic chord of the exposed tail area. In flight this tail surface pulsed continuously between stop settings of 2.76° and -3.03°.

For this model the wing plan form of aspect ratio 3 was 3.38 inches forward of the original basic wing location (ref. 11). During the burning of the rocket motor, the center of gravity of the modified wing model moved from 0.53c̄ before firing to 0.44c̄ after burnout.

TESTS

The model was boosted to a Mach number of 1.77 by a double Deacon rocket booster which separated from the model after burnout. After a slight delay, the internal rocket motor of the model fired and increased the Mach number to a maximum of 2.32. When the model was free of the booster, it was disturbed longitudinally by square-wave pulses automatically produced by the horizontal tail which changed positions from stop to stop due to the change in direction of the tail lift.

The model telemeter transmitted data throughout the test flight from instruments that measured angle of attack, angle of sideslip, total pressure, control position on stop, and normal and longitudinal accelerations. Velocity, flight path, and atmospheric data were obtained by the use of CW Doppler radar, SCR-584 tracking radar, and a rawinsonde. Flight-test Reynolds number and dynamic pressure are presented in figure 3. An envelope of the maximum angles of attack and sideslip reached by the model throughout the test flight is shown in figure 4.

Prior to the flight test the wing was statically tested to determine the chordwise wing twist due to a concentrated load along the 50-percent-chord line. Structural influence coefficients were calculated from this static test for use in estimating the loss in lift due to aeroelasticity.

ACCURACY AND CORRECTIONS

The error in the quanities from the accelerometers and air-flow indicators is approximately ±1 and ±2 percent of their calibrated instrument ranges, respectively. The calibrated ranges of the instruments used in the test model are given in the following table:

Angle-of-attack indicator, deg . . . . ±12
Angle-of-sideslip indicator, deg . . . . ±5
Normal accelerometer at the nose, g units . . . . ±40
Normal accelerometer near the center of gravity, g units . . . ±50
Longitudinal accelerometer, g units . . . . +1 to -8

Additional errors in the aerodynamic coefficients could be caused by inaccuracies in the dynamic pressure which are approximately twice as great as the errors in Mach number. The Mach number is estimated to be accurate to within ±1 percent.

Position corrections for model pitching motions were made to the angle-of-attack measurements. The readings of the normal and longitudinal

accelerometers that were located near the center of gravity were also corrected for these pitching model motions. The rate of roll was on the order of 1 radian per second throughout the Mach number range.

RESULTS AND DISCUSSION

All coefficients used herein are based on the basic wing plan form with an area of 4 square feet and a mean aerodynamic chord of 1.33 feet. The resultant data presented include any aeroelastic effects due to the flexible wing. Some corrections for aeroelasticity pertaining to normal-force-curve slope have been made and are presented in the appendix.

Drag

A typical variation of the drag coefficient with lift coefficient at a Mach number of 1.4 is shown in figure 5. The complete drag polar was plotted from the lift and drag data produced from one complete deflection cycle of the horizontal tail, that is, at stop settings of $\delta = 2.76^\circ$ and -3.03°. The drag coefficient was plotted against $C_L{}^2$ for one complete deflection cycle and the average slope was taken as the value of the drag due to lift. The minimum drag was assumed to occur at the point of zero lift.

The variation of the zero-lift drag with Mach number is presented in figure 6. It is shown here that the drag coefficient of the configuration decreases with increasing supersonic Mach number. Data from the basic wing model of reference 11, the cambered and twisted wing model of reference 5, and the body-tail model of reference 13 are also presented. The model of reference 5 has the same plan form as the model of reference 11. This comparison shows that over the comparable Mach number range the modified wing model has 6 to 8 percent less drag than the basic wing model and 11 to 17 percent less drag than the cambered and twisted wing model. Slight configuration differences, such as, wing root fairings and small accelerometer fairings on the reference models and large accelerometer fairings and lengthened fuselage on the modified model, were believed to be compensative and therefore were considered negligible in comparing drag differences. A decrease in drag by the modified wing as shown in figure 6 is also shown in the wind-tunnel tests of reference 9 for a wing-body configuration with a 6-percent-thick wing modified similarly but with inboard chords extending 67 percent forward and rearward and out to 40 percent at the semispan. Therefore, it can be noted that the addition of inboard chord-extensions can decrease the zero-lift drag of the whole configuration.

The drag due to lift of the test model, as shown in figure 7, increases steadily with Mach number. The expression $\dfrac{1}{57.3 C_{N_\alpha}}$ is slightly higher than the experimental drag due to lift throughout the Mach number range. The modified wing model with inboard chord-extensions has from 3 to 25 percent less drag due to lift in the test Mach number range above $M = 1.4$ than the basic wing model of reference 11. The drag difference between these two models increases with increasing Mach number. Comparison of the modified wing data with the cambered and twisted wing data from reference 5 shows an identical trend. A similar reduction in drag due to lift is also shown in the wind-tunnel test of reference 9 when the inboard chord modification test is compared with the basic wing test. From the present test and the reference test it can be seen that by extending the inboard wing chords forward and rearward from the wing a reduction in the drag due to lift at Mach numbers above 1.6 can be realized.

Normal-Force and Total Pitching-Moment Coefficients

The normal-force and total pitching-moment coefficients and the variation of their slopes with Mach number is presented in figures 8 to 12. Figure 8 shows that the variation of normal-force coefficient with angle of attack is linear throughout the test Mach number and angle-of-attack range. The variation of the total pitching-moment coefficient with normal-force coefficient is also linear throughout the test Mach number range and is presented in figure 9.

The variation of the normal-force-curve slope with Mach number is presented in figure 10 and shows that C_{N_α} has a gradual decrease with increasing Mach number. Along with the present test data, C_{N_α} for the basic wing model of reference 11 and C_{N_α} for the cambered and twisted wing model of reference 5 is also shown. An increase in C_{N_α} of about 0.01 over that of the basic wing model throughout the test Mach number range is apparent for the modified wing model. The normal-force-curve slope of the body-tail configuration of reference 13 is also presented in figure 10. This curve was used to determine C_{N_α} for the wing alone plus the wing-body interference by taking the difference between this curve and the normal-force-curve slope for the modified wing model. This difference is presented as the normal-force-curve slope for the elastic wing in figure 11 in order to determine the aeroelastic correction for C_{N_α}. By using the calculations from the appendix, the normal-force-curve slope of the elastic wing was corrected to the rigid wing as shown in figure 11. This correction was not applied to the data of figure 10.

The variation of the static stability parameter $\left(\dfrac{dC_m}{dC_N}\right)$ with Mach

number is presented in figure 12. The data of the modified wing model
are presented with the data of the basic wing model and the cambered and
twisted wing model. It is noted that the center of gravity of the basic
wing model and the cambered and twisted wing model are at the same posi-
tion, whereas the modified wing model has a center of gravity somewhat
forward of that position. Even though the reference data are presented
in this figure, direct comparison should not be made because of the
difference in tail length between the reference models and the present
test model whose basic wing plan form had been moved forward. At the
lower test Mach numbers the aerodynamic center of the modified wing
model has a tendency to move forward, but above a Mach number of 1.8
the value of dC_m/dC_N seems to remain constant at a value of about -0.3
based on the basic wing mean aerodynamic chord.

CONCLUSIONS

An investigation of the effects of an inboard plan-form modifica-
tion on the lift, drag, and longitudinal stability of a rocket-propelled
model having a 52.5° sweptback wing of aspect ratio 3 has been presented
herein. Analysis of the data obtained from modifying the wing plan form
by extending the inboard chord of the wing forward and rearward has pro-
duced the following conclusions:

1. The zero-lift drag of the configuration was reduced by extending
the inboard chords of the wing and thereby decreasing the inboard thick-
ness ratio.

2. Extending the inboard chords of the wing, resulted in an increase
in total lift and a reduction in drag due to lift above a Mach number of
1.6. The reduction in drag due to lift increases as Mach number increases.

Langley Aeronautical Laboratory,
    National Advisory Committee for Aeronautics,
        Langley Field, Va., April 9, 1957.

APPENDIX

EFFECTS OF WING ELASTICITY ON NORMAL-FORCE-CURVE SLOPE

An estimation of the aeroelastic effects on the normal-force-curve slope was made because of the flexibility of the thin aluminum-alloy wing. The outboard section of the modified wing would have a tendency to twist when deflected under a load because of the large sweep angle. This twist would decrease the average angle of attack of that section and therefore decrease the lift of the whole wing.

The method used to estimate the change in normal force due to the elastic deflection of the wing is explained in detail in reference 14. This method determines the ratio between the slopes of the normal-force curve for the elastic wing and the rigid wing. Wing structural influence coefficients, an assumed rigid wing spanwise lift distribution, and an estimated rigid wing normal-force-curve slope are the necessary information needed in order to estimate the elastic effects by the referenced method.

The structural influence coefficients were determined from the measured amount of twist along the wing due to static loads applied at the approximate center of pressure or, in this case, the 50-percent-chord line and at five different spanwise locations. The static test results are presented in figure 13. The assumed rigid wing spanwise lift distribution was estimated from reference 15. The normal-force-curve slope for the rigid wing was estimated by the use of the experimental wind-tunnel data of reference 9.

The results from the calculations using the referenced method are shown in figure 14 with the ratio of normal-force-curve slope for the elastic wing to that for the rigid wing plotted against the loading parameter $q\left(C_{N_\alpha}\right)_r$, where $\left(C_{N_\alpha}\right)_r$ is the normal-force-curve slope for the rigid wing.

REFERENCES

1. Brown, Clinton E., and Hargrave, L. K.: Investigation of Minimum
   Drag and Maximum Lift-Drag Ratios of Several Wing-Body Combinations
   Including a Cambered Triangular Wing at Low Reynolds Numbers and at
   Supersonic Speeds. NACA RM L51E11, 1951.

2. Cohen, Clarence B.: Influence of Leading-Edge Suction on Lift-Drag
   Ratios of Wings at Supersonic Speeds. NACA TN 1718, 1948.

3. Burrows, Dale L., and Palmer, William E.: A Transonic Wind-Tunnel
   Investigation of the Longitudinal Force and Moment Characteristics
   of a Plane and a Cambered 3-Percent-Thick Delta Wing of Aspect
   Ratio 3 on a Slender Body. NACA RM L54H25, 1954.

4. Burrows, Dale L., and Tucker, Warren A.: A Transonic Wind-Tunnel
   Investigation of the Static Longitudinal Characteristics of a
   3-Percent-Thick, Aspect-Ratio-3, Delta Wing Cambered and Twisted
   for High Lift-Drag Ratios. NACA RM L55F02a, 1955.

5. Gillespie, Warren, Jr.: Effect of Wing Camber and Twist at Mach
   Numbers From 1.4 to 2.1 on the Lift, Drag, and Longitudinal Sta-
   bility of a Rocket-Powered Model Having a 52.5° Sweptback Wing
   of Aspect Ratio 3 and Inline Tail Surfaces. NACA RM L56C16, 1956.

6. Polhamus, Edward C.: Drag Due to Lift at Mach Numbers up to 2.0.
   NACA RM L53I22b, 1953.

7. Hall, Charles F.: Lift, Drag, and Pitching Moment of Low-Aspect-
   Ratio Wings at Subsonic and Supersonic Speeds. NACA RM A53A30,
   1953.

8. Bielat, Ralph P., Harrison, Daniel E., and Coppolino, Domenic A.:
   An Investigation at Transonic Speeds of the Effects of Thickness
   Ratio and of Thickened Root Sections on the Aerodynamic Character-
   istics of Wings With 47° Sweepback, Aspect Ratio 3.5, and Taper
   Ratio 0.2 in the Slotted Test Section of the Langley 8-Foot High-
   Speed Tunnel. NACA RM L51I04a, 1951.

9. Cooper, Morton, and Sevier, John R., Jr.: Effects of a Series of
   Inboard Plan-Form Modifications on the Longitudinal Characteristics
   of Two 47° Sweptback Wings of Aspect Ratio 3.5, Taper Ratio 0.2,
   and Different Thickness Distributions at Mach Numbers of 1.61 and
   2.01. NACA RM L53E07a, 1953.

10. Sevier, John R., Jr.: Investigation of the Effects of Body Indenta-
     tion and of Wing-Plan-Form Modification on the Longitudinal Char-
     acteristics of a 60° Swept-Wing—Body Combination at Mach Numbers
     of 1.41, 1.61, and 2.01. NACA RM L55E17, 1955.

11. Gillespie, Warren, Jr.: Lift, Drag, and Longitudinal Stability at
     Mach Numbers From 1.4 to 2.3 of a Rocket-Powered Model Having a
     52.5° Sweptback Wing of Aspect Ratio 3 and Inline Tail Surfaces.
     NACA RM L55I12, 1955.

12. Gillespie, Warren, Jr., and Dietz, Albert E.: Use of an Aerody-
     namically Pulsed All-Movable Horizontal Tail to Obtain Longitu-
     dinal Characteristics of Rocket-Powered Models in Free Flight
     and Some Initial Results From an Arrow-Wing-Body-Tail Configuration.
     NACA RM L52C10, 1952.

13. Gillespie, Warren, Jr., and Dietz, Albert E.: Rocket-Powered Model
     Investigation of Lift, Drag, and Stability of a Body-Tail Con-
     figuration at Mach Numbers From 0.8 to 2.3 and Angles of Attack
     Between ±6.5°. NACA RM L54C04, 1954.

14. Vitale, A. James: Effects of Wing Elasticity on the Aerodynamic
     Characteristics of an Airplane Configuration Having 45° Sweptback
     Wings As Obtained From Free-Flight Rocket-Model Tests at Transonic
     Speeds. NACA RM L52L30, 1953.

15. Cohen, Doris, and Friedman, Morris D.: Theoretical Investigation
     of the Supersonic Lift and Drag of Thin, Sweptback Wings With
     Increased Sweep Near the Root. NACA TN 2959, 1953.

TABLE I.- CONTOUR ORDINATES OF NOSE

Station, in. from nose	Body radius, in.
0	0.17
.06	.18
.12	.21
.24	.22
.48	.28
.73	.35
1.22	.46
2.00	.64
2.45	.73
4.80	1.24
7.35	1.72
8.00	1.85
9.80	2.15
12.25	2.50
13.12	2.61
14.37	2.75
14.70	2.78
17.15	3.01
19.60	3.22
22.05	3.38
24.50	3.50
25.00	3.50

DECLASSIFIED

TABLE II.- GEOMETRIC AND MASS CHARACTERISTICS OF MODEL

Wing:
  Span, ft 3.46
  Area, sq ft
    Basic wing 4.00
    Modified wing 6.49
  Aspect ratio
    Basic wing 3.00
    Modified wing 1.85
  Taper ratio
    Basic wing 0.20
  Sweepback of 0.25 chord, deg
    Basic wing 52.50
    Modified wing
      Inboard panel 65.00
      Outboard panel 52.50
  Sweepback of 0.50 chord, common to both wings, deg 47.50
  Mean aerodynamic chord, ft
    Basic wing 1.33
    Modified wing 2.86
  Airfoil section
    Basic wing . . . . NACA 65A004
    Modified wing
      At 0.5b/2 to tip . . . . NACA 65A004
      At wing-body juncture . . . . NACA 65A002
  Wing thickness at center line, percent chord 1.76

Body:
  Maximum diameter, ft 0.58
  Base diameter, ft 0.42
  Length, ft 10.16
  Fineness ratio 17.41
  Boattail angle, deg 2.16

Horizontal tail:
  Span, ft 1.85
  Aspect ratio 2.70
  Sweepback of 0.50 chord, deg 0
  Airfoil section . . . . 4 percent hexagonal

Vertical tail:
  Span, ft 1.67
  Aspect ratio 1.18
  Sweepback of leading edge, deg 70
  Sweepback of trailing edge, deg 15
  Airfoil section . . . . $\frac{1}{4}$-inch beveled flat plate

Model weight, lb:
  With rocket motor loaded 190.0
  With rocket motor empty 145.8

Moment of inertia in pitch, slug-ft^2:
  With rocket motor loaded 32.86
  With rocket motor empty 29.19

Center of gravity, percent of mean aerodynamic chord:
  With rocket motor loaded
    Basic wing $\bar{c}$ 53
    Modified wing $\bar{c}$ 57
  With rocket motor empty
    Basic wing $\bar{c}$ 44
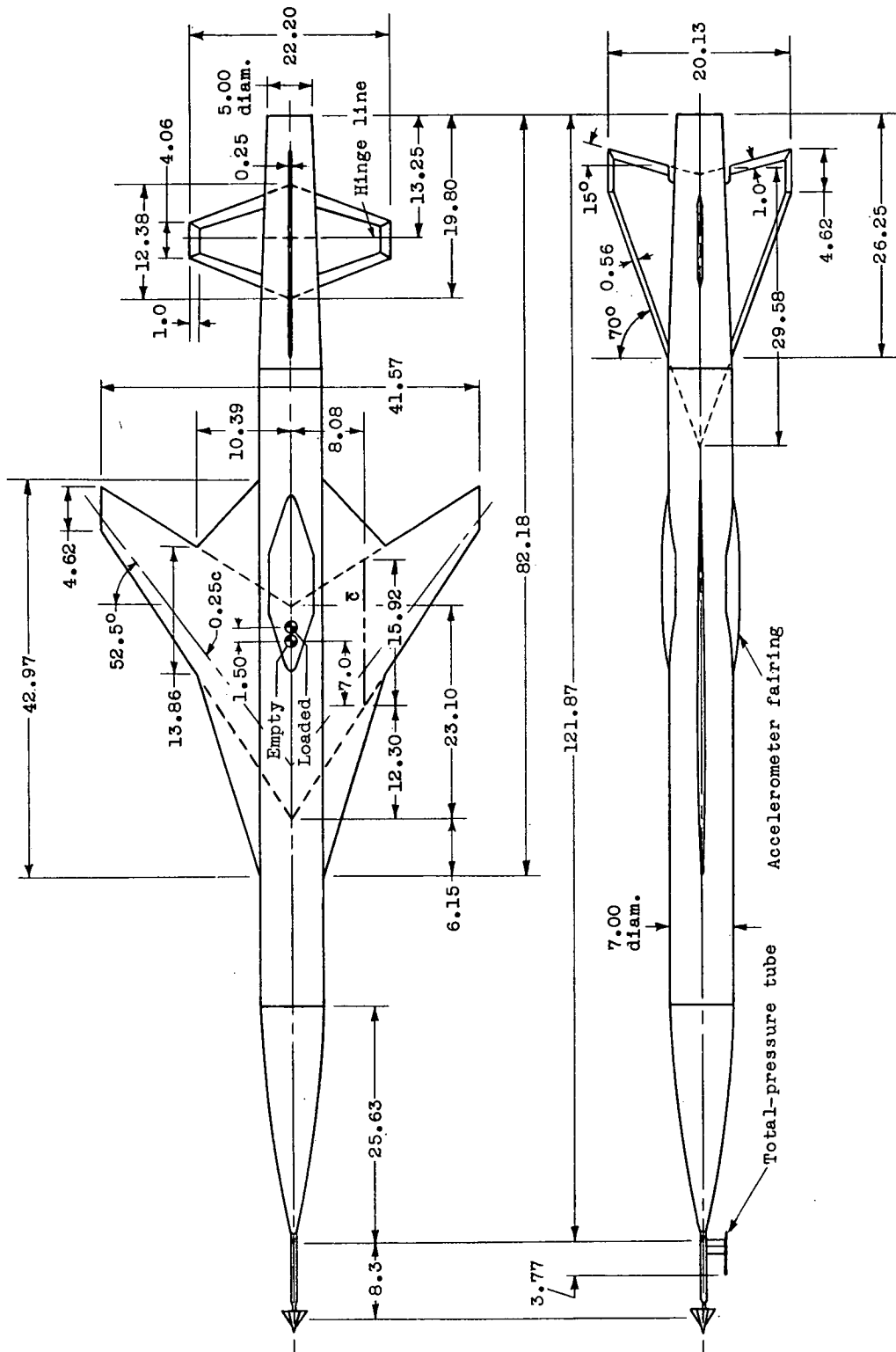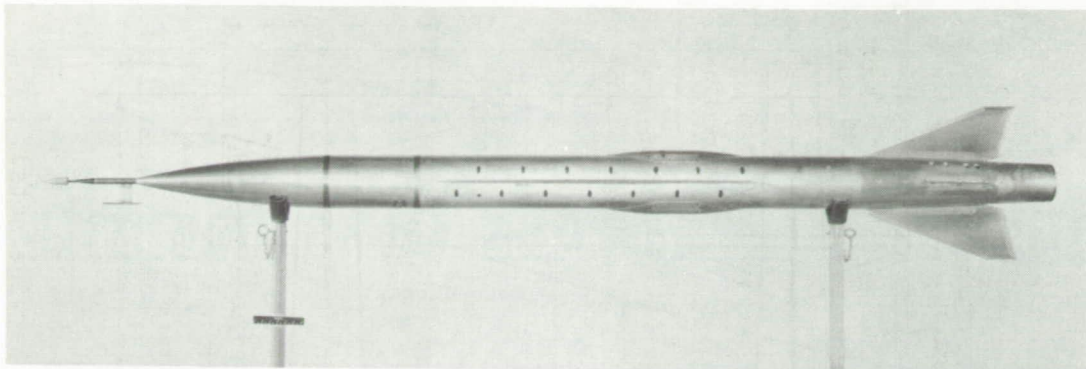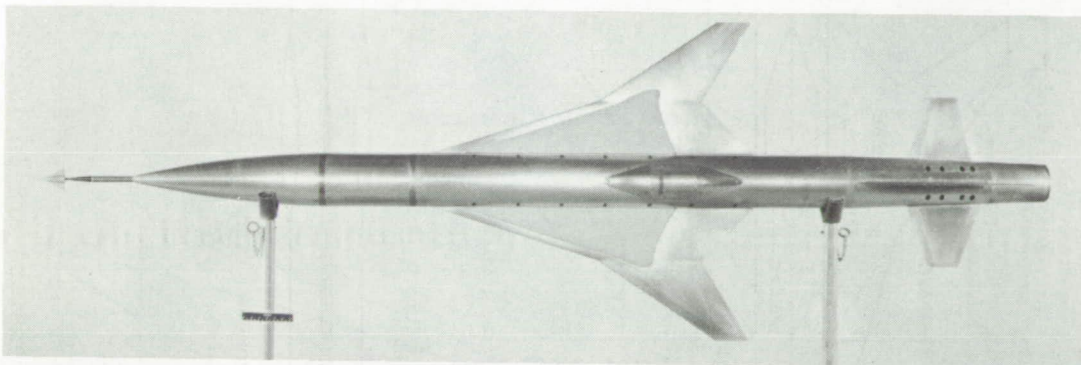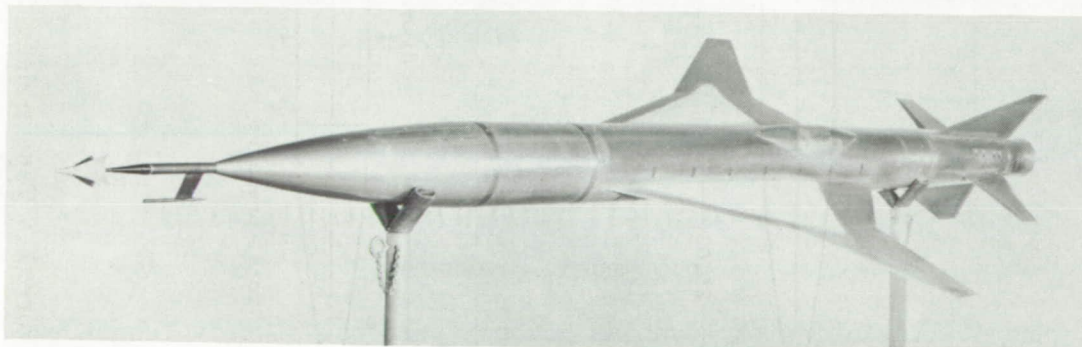   Modified wing $\bar{c}$ 52

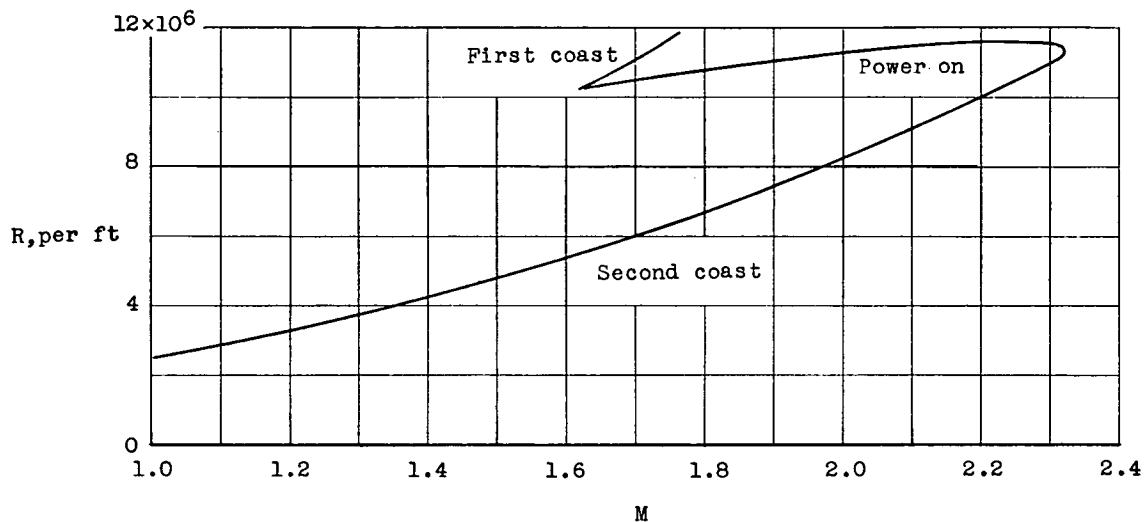Figure 1.- Test model. All dimensions are in inches unless otherwise noted.
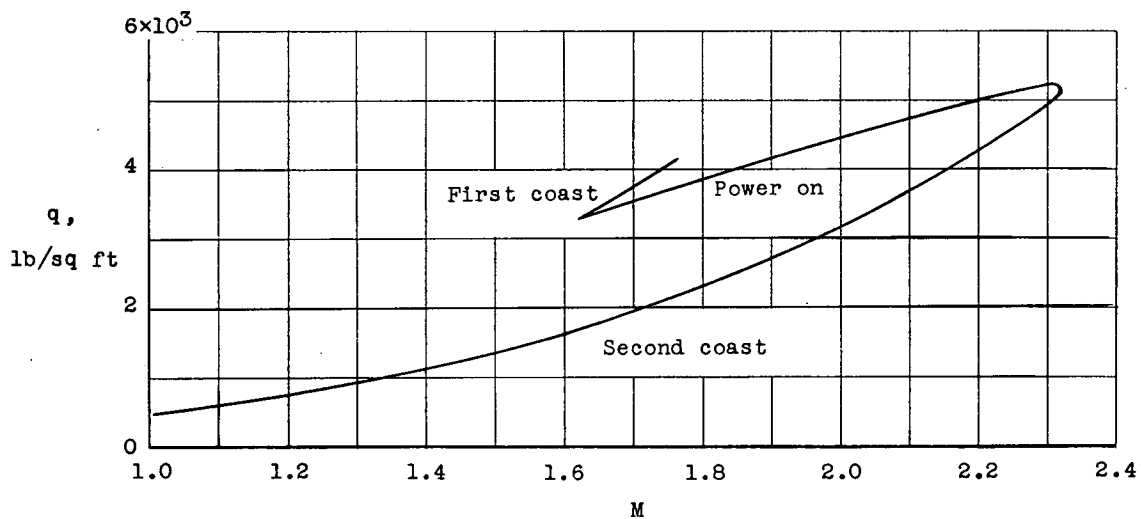
(a) Side view.

(b) Top view.

(c) Three-quarter view.   L-57-1556

Figure 2.- Photographs of model.

CONFIDENTIAL NACA RM L57D29

(a) Reynolds number.

(b) Dynamic pressure.

Figure 3.- Variation of Reynolds number, per foot of body length, and dynamic pressure with Mach number.

DECLASSIFIED
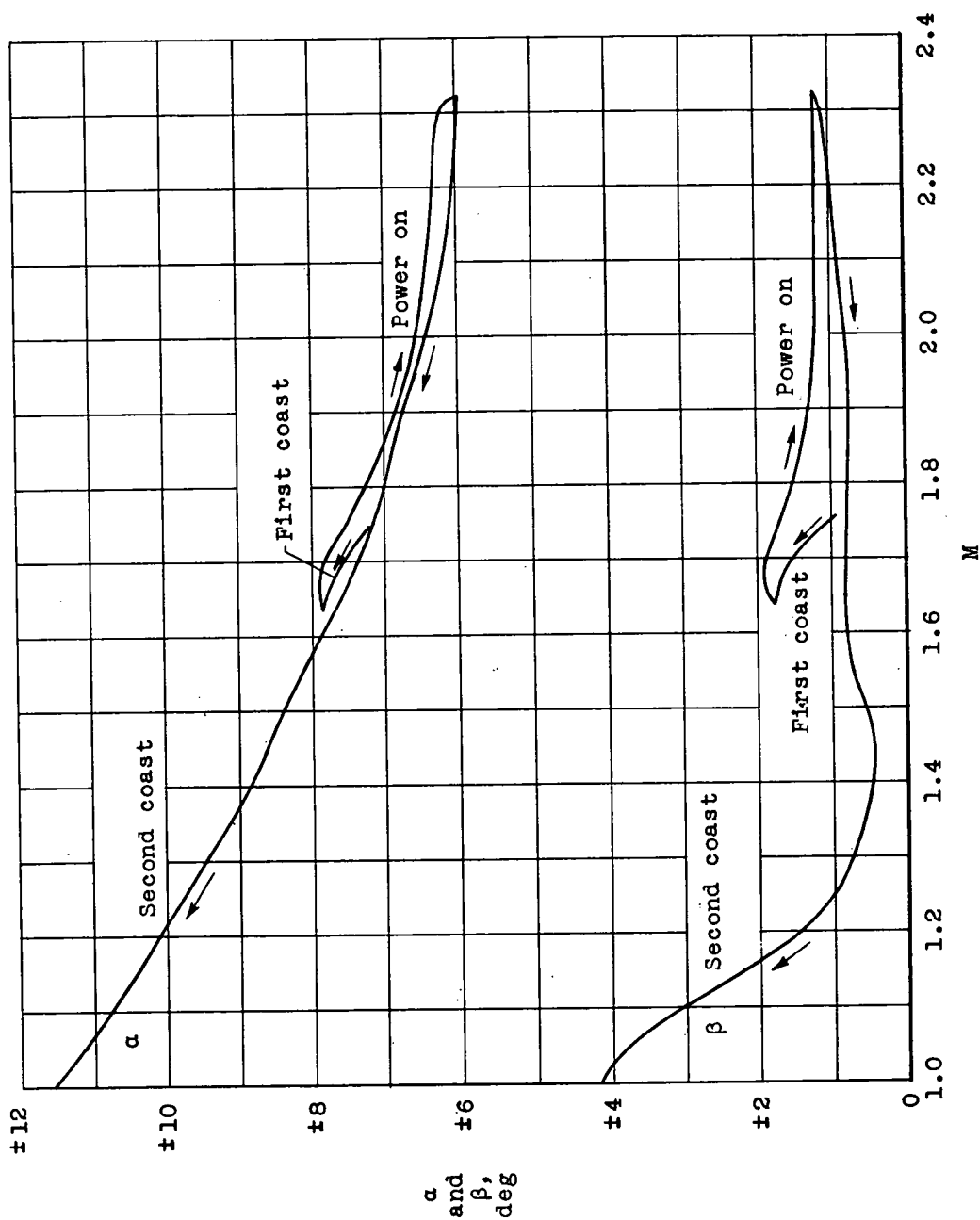
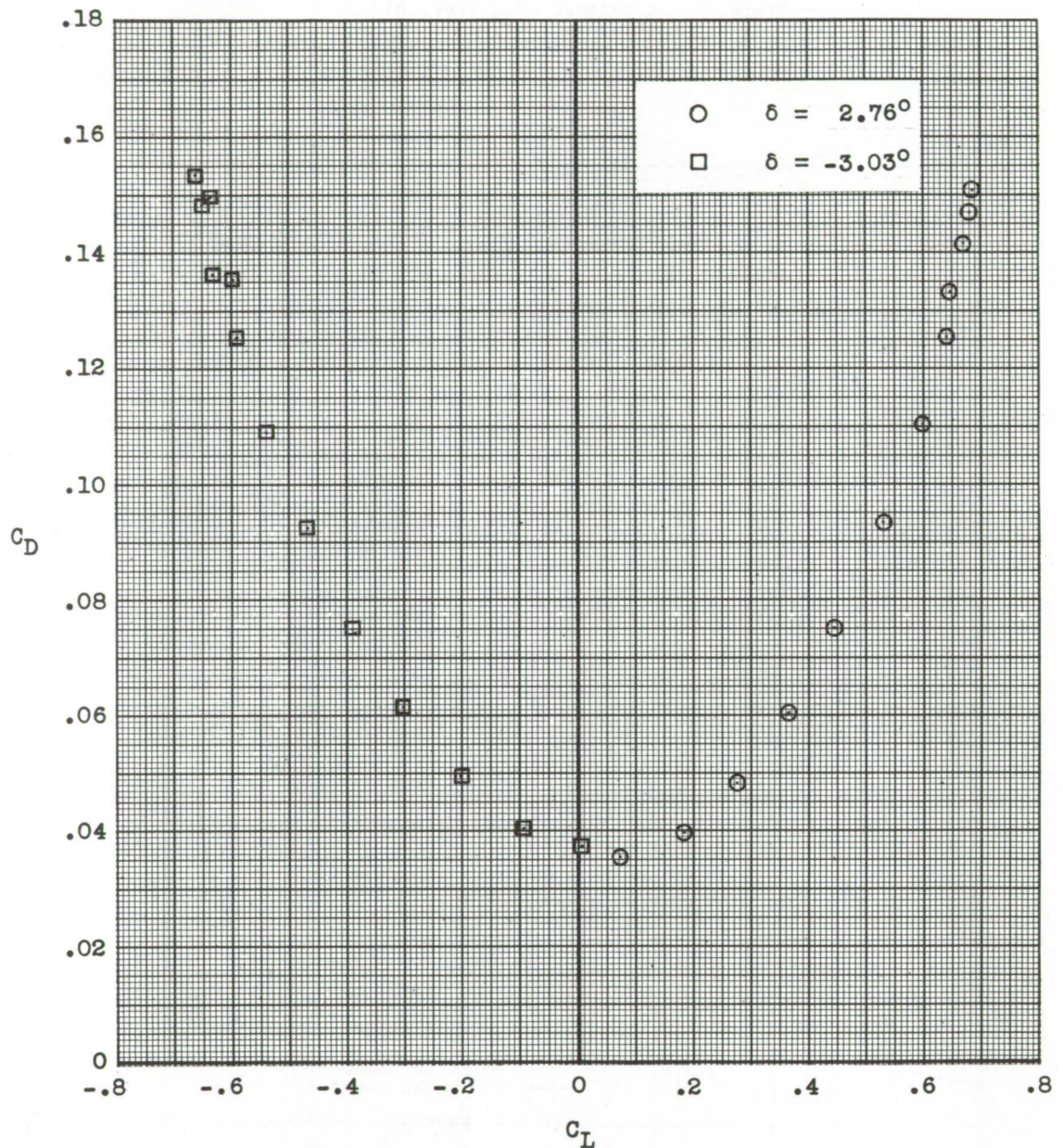Figure 4.- Variation of maximum angle of attack and induced sideslip with Mach number.

Figure 5.- Typical variation of drag coefficient with lift coefficient. Mach number, 1.4.

Figure 6.- Variation of zero-lift drag coefficient with Mach number.

Figure 7.- Variation of drag due to lift with Mach number.

CONFIDENTIAL

Figure 8.- Typical variation of normal-force coefficient with angle of attack over the Mach number range.

Figure 9.- Typical variation of pitching-moment coefficient with normal-force coefficient over the Mach number range.

Figure 10.- Variation of the normal-force-curve slope with Mach number.

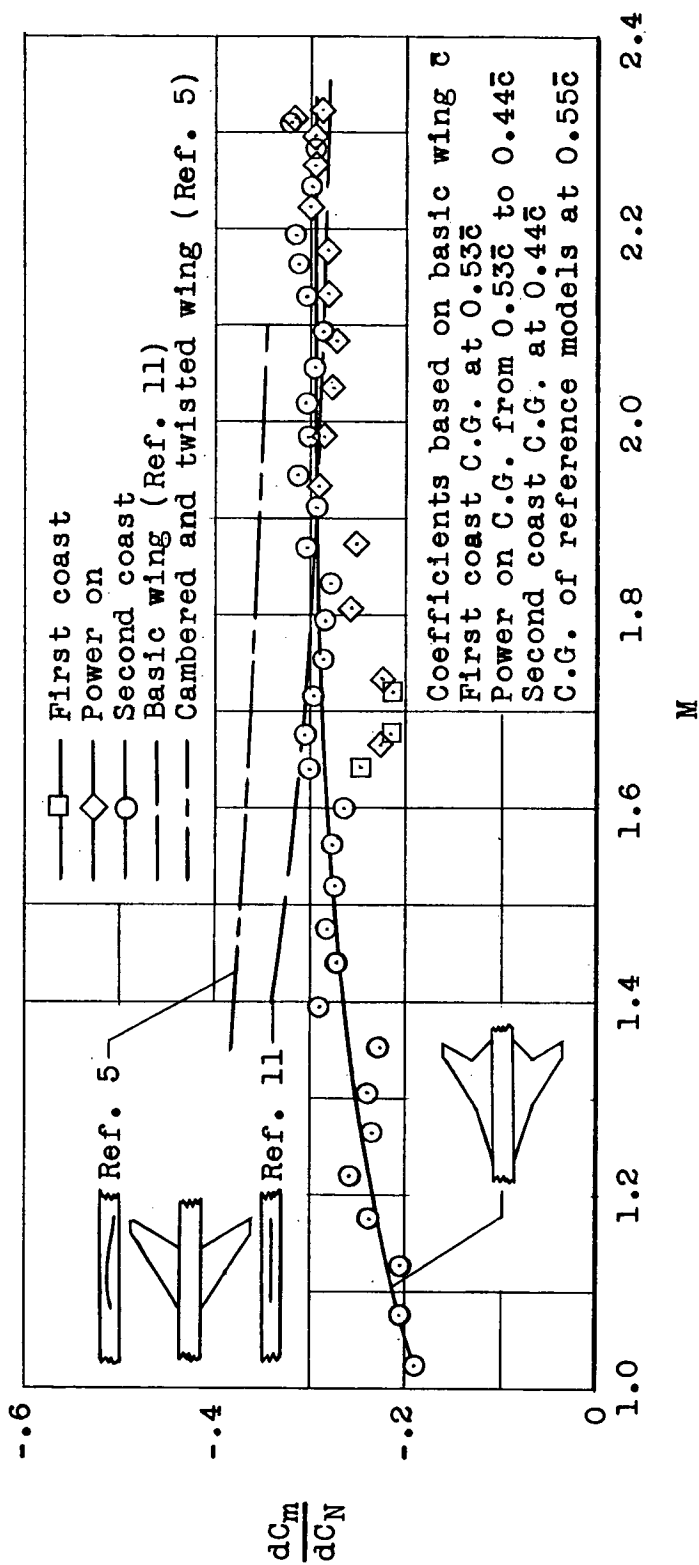Figure 11.- Variation of the wing normal-force-curve slope with Mach number. Wing alone with interference.

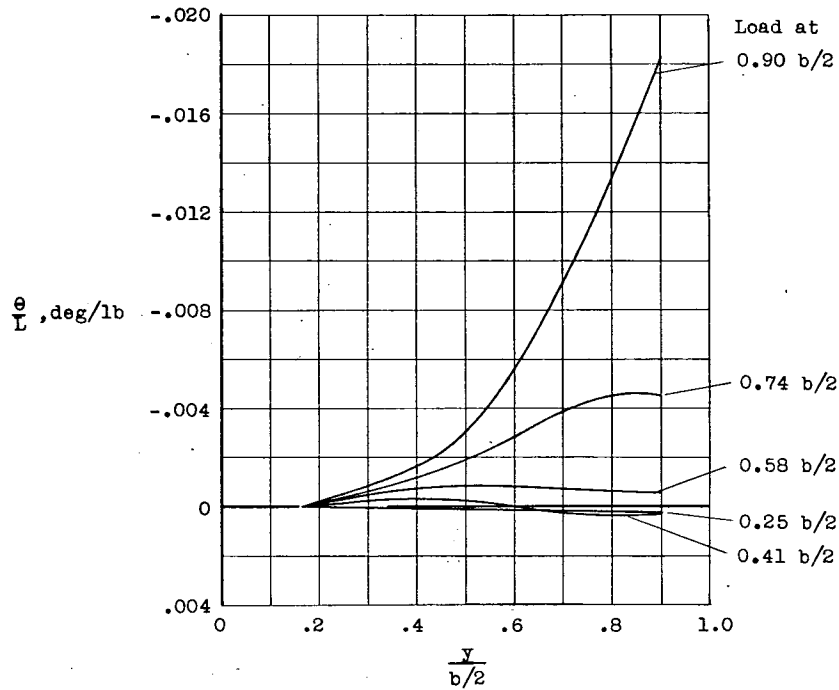Figure 12.- Variation of static stability parameter with Mach number.

$\frac{\theta}{L}$,deg/lb

Load at 0.90 b/2

0.74 b/2

0.58 b/2

0.25 b/2

0.41 b/2

$\frac{y}{b/2}$

Figure 13.- Streamwise wing twist due to 1-pound load at 0.50 chord.

$\frac{(c_{N_\alpha})_e}{(c_{N_\alpha})_r}$

$q\ (c_{N_\alpha})_r$

Figure 14.- Calculated ratio of normal-force-curve slope for the elastic wing to that for the rigid wing.